

Thermal Inspection and Quality Assessment for AFP Processes via Automatic Defect Detection and Segmentation

Muhammed Zemzemoglu and Mustafa Unel

Faculty of Engineering and Natural Sciences, Sabanci University, Istanbul, Turkey

Integrated Manufacturing Technologies Research and Application Center, Sabanci University, Istanbul, Turkey

{mzamzam,munel}@sabanciuniv.edu

Abstract—Automated fiber placement (AFP) technology, while highly beneficial, is susceptible to defects that compromise the final product’s mechanical integrity. Traditional manual inspection methods are labor-intensive, error-prone, and result in significant downtime. This study introduces an innovative framework for AFP process inspection and quality assessment using thermal imaging, machine learning algorithms, and computer vision techniques. The system comprises defect detection, defect segmentation, and quality assessment components. By providing real-time feedback, it offers qualitative defect attributes (shape, size, and location) and a novel quantitative defect impact metric. An active knowledge-driven decision support system (AFP-DSS) aids operator maintenance and repair decisions. Experimental validation shows the defect detection component achieving 96.4% accuracy with a 2.8% false negative rate, and the defect segmentation component attaining 93.2% mean pixel accuracy and a mean Intersection over Union (IoU) score of 0.72. Operating in real-time, the system effectively reduces machine downtime, enhances production quality, and improves the economic viability of AFP technology.

Index Terms—automated fiber placement, thermographic inspection, quality assessment, defect detection and segmentation, decision support system, computer vision, machine learning.

I. BACKGROUND AND RELATED WORK

Automated Fiber Placement (AFP) technology has transformed composite material construction, evolving from traditional methods like hand lay-up (HLU) and automated tape lay-up (ATL) to achieve greater speed and precision. AFP involves the precise, layer-by-layer placement of fibers into a mold, enhancing structural integrity and production efficiency, particularly in the aerospace industry. Recent studies highlight that AFP technology accounts for approximately 50% of all aerospace composite construction, underscoring its significant impact [1].

Despite its advantages, AFP is prone to defects such as gaps, overlaps, missing tows, tow splices, and foreign bodies, which can compromise the mechanical strength and reliability of the final product. Unresolved defects not only deviate from design requirements but also elevate the risk of part failure [2]. Additionally, AFP systems face productivity and cost challenges due to high downtime associated with quality inspection and defect repair cycles. A recent survey revealed that AFP systems may spend up to 42% of their work time

on inspection tasks compared to only 19% on actual lay-up, highlighting the need for an automated solution [3].

Manual inspection in AFP processes is time-consuming, labor-intensive, and prone to human error, necessitating frequent interruptions for defect detection and correction. Missed defects during manual inspection can lead to significant challenges during post-curing stages. An automatic in-process monitoring and inspection module promises to address these issues by enabling real-time inspection and quality assessment, thereby improving productivity and reducing costs.

Various technologies have been explored for AFP monitoring but often are limited to off-process applications [4]. Machine vision systems, especially thermal imaging, show promise in in-situ inspection by enhancing visibility during AFP’s preheating step [5]. Studies confirm that thermography-based AFP monitoring outperforms traditional methods like profilometry and visible inspection [6]. Machine learning (ML) has also improved defect detection and segmentation accuracy in AFP monitoring [7]. Despite these advances, data scarcity and solution reliability remain challenges. Hybrid approaches combining computer vision and ML techniques show promise in addressing these issues. For instance, integrating classical algorithms with deep learning networks has proven effective in segmenting and clustering defect points [8].

Despite technological progress, there is no comprehensive end-to-end quality assessment and process inspection system for AFP. This study introduces an innovative automatic monitoring and quality inspection system for AFP processes, utilizing thermal imaging and ML algorithms alongside computer vision techniques. The system includes three main components: defect detection, defect segmentation, and quality assessment. It lays the foundations for an active decision support system by providing real-time feedback, including qualitative defect attributes—such as shape, size, and location—and a novel quantitative defect impact evaluation metric. Additionally, a dynamic knowledge base with alert/recommendation pairs is included, offering continuous improvement in decision support based on expert insights and real-time data. The proposed solution aims to reduce machine downtime, enhance production efficiency, and improve the economic viability of AFP technology.

II. DATA DESCRIPTION AND EXPERIMENTAL SETUP

A. Data Acquisition

The experiments were conducted using a Coriolis C1 AFP machine. A FLIR A655sc thermal camera captured images at 640×480 pixels and 50 frames per second. A spatial calibration was carried out to correct for any distortions introduced by the camera and lens. Positioned using a previously developed in-situ vision system [9], the camera's images were streamed to a workstation equipped with an Intel Xeon W-2275 14-core CPU and an NVIDIA Quadro RTX 5000 GPU for processing.

Experiments were conducted under various process and environmental conditions, as outlined in Table I. The data acquisition frequency was preset based on lay-up speed using a trigger mechanism. At the standard lay-up speed, the acquisition rate was set to 5 Hz, corresponding to a pitch size of $\alpha = 12$ mm. For real-time operation, the maximum allowable processing time for the entire pipeline is $\tau = 200$ ms.

B. Preprocessing and Database Overview

Due to the lack of publicly available thermal imaging databases for AFP process defects, we utilized a previously constructed in-house database and followed the same pre-processing pipeline as described in [10]. This database was developed from experiments conducted under various acquisition conditions and process parameters. While this provides a comprehensive dataset, potential challenges include new scenarios due to variability in material properties, environmental conditions, and equipment calibration. To address these challenges, the dynamic structure of our system enables continuous enrichment of the database with new lay-up instances, thereby increasing its robustness and applicability.

The database is categorized into two main classes: Healthy lay-up (H) and Defective lay-up (D). The Defective class is further divided into five distinct subclasses: Gaps (G), Overlaps (O), Missing Tows (MT), Tow Splices (TS), and Foreign Bodies (FB). To enrich the database, domain-specific augmentation techniques were applied, resulting in a total of 5,000 manually labeled images. This includes 2,500 images for the Healthy class and 500 images for each defect subclass. A key contribution of this study is conducting new experiments to increase real data, enhancing the model's reliability.

TABLE I
AFP PROCESS AND ENVIRONMENT PARAMETERS

Parameter Type	Value(s)/Interval
Material temperature	$20^\circ - 28^\circ\text{C}$
Tool surface temperature	$32^\circ - 50^\circ\text{C}$
Ambient temperature	$19^\circ - 24^\circ\text{C}$
Compaction pressure	3 – 6 bar
Number of layers	1 – 6
Number of tows	4
Lay-up angles	$0^\circ, 45^\circ, 90^\circ$
Nominal lay-up speed	0.25 m/s
Prepreg material	Thermoset
Tow width	6.35 mm
Tow thickness	$160 \mu\text{m}$

III. METHODOLOGICAL FRAMEWORK

A. System Architecture

The proposed system architecture consists of three main components divided into two blocks: operational and decision support. The operational block handles automated inspection and analysis, while the decision support block processes findings for high-level quality assessments, aiding maintenance and repair decisions.

Designed for real-time operation and efficiency, the operational block first tests a lay-up for defects and proceeds to the computationally intensive defect segmentation only if defects are detected, conserving resources and facilitating smoother operation. We adopt an integrated approach, utilizing a combination of machine learning algorithms and computer vision techniques to optimize performance and efficiency. The decision support component integrates findings from the detection and segmentation modules, presenting them in a real-time process monitoring stream and generating informed decisions based on an alert/recommendation knowledge base.

The architecture and flow of the system are illustrated in Fig. 1. Initially, a test thermal image is preprocessed, added to the database, and fed into the operational block. The defect detection component automates the manual detection process, reducing machine downtime. Each input image is classified as 'healthy' or 'defective'.

If a lay-up is flagged as 'defective', the subsequent defect characterization component is activated and an advanced defect segmentation algorithm is employed to classify the defect region at the pixel level, extracting features such as shape, size, and location. These outputs are then used to evaluate lay-up quality, assess the defect's impact, and assist the decision of the operator.

The synergistic integration of these system components forms the foundation of the Automated Fiber Placement process decision support system (AFP-DSS). This comprehensive approach ensures precise identification, characterization, and evaluation of defects, enabling timely, well-informed decision-making for enhanced AFP process monitoring and quality inspection. The following subsections delve into the technical specifics of each component, illustrating their crucial roles in improving overall quality and addressing the research problem.

B. Enhanced Defect Detection

This component classifies lay-up status by detecting defects in a binary classification setup. Building on our previous work [10], we introduce three key enhancements: temperature normalization before Gabor filter extraction, adoption of a non-linear kernel in the Support Vector Machine (SVM) classifier, and training on a richer dataset with a higher percentage of original defective instances. These enhancements are shown to improve detection accuracy, robustness, and generalizability.

1) *Temperature Normalization*: While preprocessing ensures spatial alignment, temporal alignment challenges remain, affecting performance and interpretability. Previously deposited regions exhibit higher temperatures, resulting in a

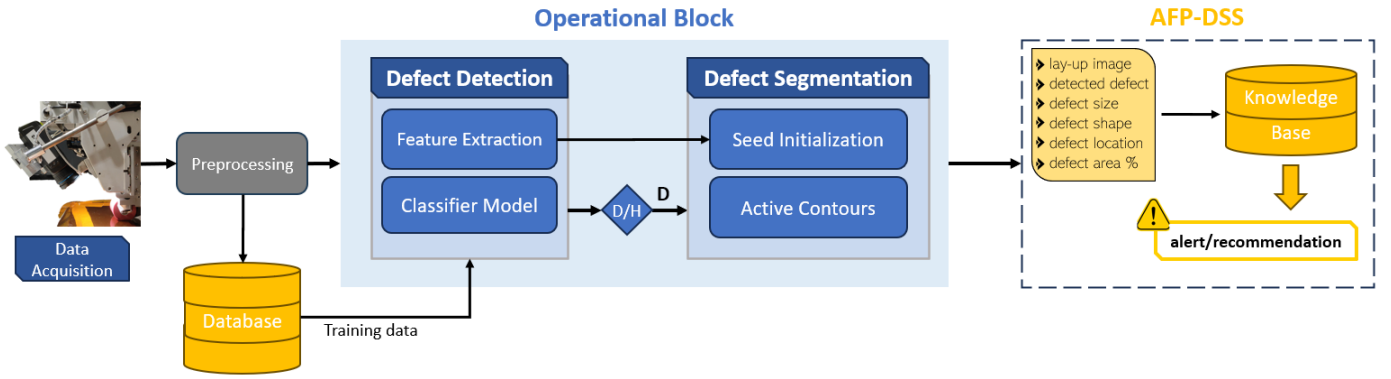


Fig. 1. A schematic diagram illustrating the architecture of the proposed thermal inspection and quality assessment framework.

gradient pattern due to varying heat exposure durations. To mitigate this, we calculate the average temperature across the width of each course and subtract it from the preprocessed image, achieving both spatial and temporal alignment. Fig. 2 shows the impact of this step with more distinct defect manifestations. Post-normalization, the enhanced visual clarity facilitates efficient process monitoring and easier database labeling. This step also improves the overall performance of the operational block components. Gabor filters are then applied for feature extraction, creating feature vectors used as input for the SVM classifier.

2) *RBF-Kernel Based SVM Classifier*: The SVM implementation adopts a soft-margin approach to handle non-linearly separable data. The kernel trick allows the SVM to operate in a higher-dimensional space without explicit transformation, enhancing efficiency. Despite the relatively high computational cost, we employ a Radial Basis Function (RBF) kernel due to its superior capability in managing nonlinear feature relationships and its exceptional performance in image-based classification tasks [11]. The RBF kernel equation is presented below:

$$K(\mathbf{x}_i, \mathbf{x}_j) = \exp(-\gamma \|\mathbf{x}_i - \mathbf{x}_j\|^2) \quad (1)$$

In this equation, \mathbf{x}_i and \mathbf{x}_j are feature vectors, and γ is the kernel's control parameter, which adjusts the complexity of the

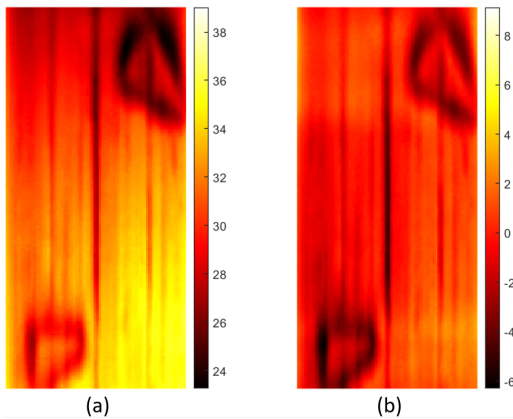


Fig. 2. Temperature normalization: (a) raw thermal image of flawless lay-up, (b) temperature-normalized version showing relative temperature differences from the average.

decision boundary. The designed soft-margin SVM, employing an RBF kernel, is trained on feature vectors extracted from the temperature-normalized database images.

The RBF kernel enhances the classifier's ability to address non-linear relationships, thereby improving its overall classification accuracy. As the manufacturing process evolves, new training data can be effortlessly added to the database, demonstrating a key benefit of learning-based methods. To achieve optimal performance, a grid search technique is employed for parameter tuning. After optimization, the model is prepared to classify real-time images as either 'Defective' or 'Healthy'.

C. Defect Segmentation and Localization

Upon detecting a defect, the segmentation algorithm isolates defective region pixels from the healthy background in real-time. Previous studies used various approaches for AFP defect segmentation, including masking, thresholding, region growing, watershed, clustering, and graph-based algorithms [12]. We developed an active contours segmentation algorithm using Gabor texture features as seeds, enhancing performance without additional computational burden since these features are applied in both detection and segmentation.

1) *Seed Initialization with Texture Features*: As an initial step, we compute the mean image of healthy lay-up instances from our temperature-normalized database and subtract it from defective images. This normalization reduces eliminate static biases and consistent background variations, enhancing defect identification and isolation. The selection of seed features in the active contours algorithm can range from edge pixels (edgels) to more advanced image features, and this choice is closely linked to the algorithm's performance. Gabor filters have been found to outperform other feature types in fabric-based defect detection and segmentation applications, making them the feature extraction method of choice for our proposed algorithm [13]. Gabor filters are considered a simplified yet effective model that approximates human texture perception.

2) *Active Contours Evolution*: The active contours algorithm begins with an initial contour that iteratively evolves to enclose the defective region. Compared to other image segmentation techniques, active contours, when initialized with appropriate seeds, demonstrate superior performance. This approach was successfully validated in segmenting thermal

images of a uniform specimen [14], and is extended in this work to the more complex task of defect segmentation in AFP thermal lay-up images. By utilizing Gabor texture features to initialize the algorithm instead of using random seeds, we ensure enhanced segmentation accuracy and faster convergence. During each iteration, the active contour deforms based on forces derived from image features, including Gabor features, and internal constraints that maintain contour smoothness, thereby minimizing an energy function. This function is designed to balance maintaining a smooth contour with accurately fitting the defective region.

Our proposed active contours algorithm employs the Chan-Vese region-based energy model, as detailed in [15]. Although the algorithm is computationally intensive, the use of pre-computed feature vectors for initialization and the relatively low resolution of the images help mitigate these computational demands. As the contour converges, the defective region is precisely isolated from the background and labeled accordingly.

D. Quality Assessment and Decision Support System

The primary objective of this component is to evaluate defective lay-ups, assessing defects from multiple perspectives and presenting results in a meaningful format. Instead of extracting new characteristics, it processes findings into a high-level format for AFP quality assessment. We establish an active knowledge-driven decision support system (AFP-DSS) that generates maintenance and repair suggestions. This DSS uses expert knowledge, rules, and heuristics to support decision-making by matching the current situation to a pre-defined knowledge base. Each lay-up configuration is linked to an alert or recommendation pair based on expert insights [16].

The defect segmentation algorithm extracts critical spatial information about the defect region, including shape, size, and location. We introduce a novel numerical metric based on this spatial information for defect impact evaluation. This framework supports both qualitative and quantitative evaluation, enabling the development of a robust alert/recommendation knowledge base. Emphasizing interpretability and transparency, the AFP-DSS presents its outputs in real-time through a user-friendly interface.

1) *Quantitative Assessment Metric:* We propose a novel metric to assess the local impact of defects, defined as the ratio of defect pixels to the total pixels within the affected horizontal lay-up area. This definition is tailored to the specific nature of AFP production, where defects primarily affect the cross-sectional direction. This metric categorizes defects by severity, tracks trends over time, and prioritizes defects for repair. Larger defect areas are critical as they significantly compromise structural integrity. To enhance accuracy, pixel-wise area evaluations are converted to real-world coordinates using camera calibration. This metric is central to the alert/recommendation knowledge base, aligning with qualitative results from other system components to comprehensively evaluate the lay-up status and ensure robust production quality assessment.

true label	Defective (+)	0.97	0.03
	Healthy (-)	0.05	0.95
		Defective (+)	Healthy (-)
		predicted label	

Fig. 3. Normalized confusion matrix for SVM test set classification results.

IV. RESULTS AND DISCUSSION

A. Defect Detection Results and Evaluation

The classifier model’s performance was evaluated following the described enhancements. The updated database was divided into training (80%), validation (10%), and testing (10%) subsets for model training and optimization. During training and validation, a grid search algorithm determined the optimal model parameters. Emphasis was placed on achieving high recall (sensitivity) due to the critical impact of undetected defects on production quality. No overfitting was observed when comparing training and test dataset performances; thus, our analysis focuses on the test set’s performance. Test set results are shown in a confusion matrix (Fig. 3), juxtaposing predicted and actual class labels, with ‘Defective’ as positive and ‘Healthy’ as negative.

The performance of the enhanced model was assessed using accuracy, precision, recall, and F1-score. The model parameters and performance metrics are shown in Table II. The enhanced model achieved classification accuracies of 97.2% for defective and 95.6% for healthy lay-up classes. Minimizing false negative rate is vital, as misclassifying a defective instance endangers part’s mechanical integrity. With a false negative rate of 2.8%, the model reliably detects most defects. Additionally, the low false positive rate of 4.4% reduces unnecessary machine stops, minimizing downtime and costs.

The model achieved a high test accuracy of 96.4% and an F1-score of 96.43%, highlighting its strong predictive performance in distinguishing defective from healthy lay-ups. Although the percentage improvements might seem incremental, it is crucial to highlight that these results were obtained using a significantly richer database. This substantial improvement in data quality enhances the credibility and reliability of the results, underscoring the robustness of the enhanced model in practical applications. Misclassifications likely arise from similarities in features between different entities in the images, such as the width of hotter regions distinguishing gaps from tow boundaries. Incorporating a conditional statement into the system could mitigate this confusion.

The SVM model is efficient, with most of the processing load in the feature extraction step, resulting in an average total processing time of 72.7 ms. Although the Gabor filter bank is pre-generated and reused, convolving each filter with the lay-up image consumes considerable runtime. However, the time requirements remain acceptable since these features are reused

in the defect segmentation component. The algorithm’s average execution time per image is 89.7 ms , making it suitable for real-time AFP process monitoring. Overall, the SVM model demonstrates robust generalization and efficiency, providing reliable classification for AFP lay-up status monitoring.

B. Defect Segmentation Performance

The effectiveness of the defect segmentation and localization algorithm is critical for accurate processing. We evaluate its performance using pixel-wise accuracy (PA%) and intersection over union (IoU) metrics: PA% measures the percentage of correctly classified pixels compared to the ground truth, while IoU measures the overlap between the predicted segmentation and the ground truth:

$$PA\% = \left(\frac{TP + TN}{TP + TN + FP + FN} \right) \times 100 \quad (2)$$

$$IoU = \frac{|S \cap G|}{|S \cup G|} \quad (3)$$

Here TP denotes true positives, TN true negatives, FP false positives, and FN is false negative. In the IoU formula, $|S \cap G|$ represents the intersection of the predicted segmentation and the ground truth, while $|S \cup G|$ represents their union.

We first demonstrate the algorithm’s performance on a selected example, showcasing initialization and contour evolution, and later evaluate its mean accuracy using the mentioned metrics and execution time. Foreign bodies and tow splices, due to their similar thermal characteristics and complex shapes, are particularly challenging to segment. To rigorously assess the algorithm, we present a case study focusing on a lay-up image featuring a foreign body. This scenario tests the algorithm’s ability to segment and localize defects amidst image noise, providing a comprehensive evaluation of its real-world effectiveness.

The active contours algorithm with texture feature seeds was applied to the same case study for comparison. Fig. 4 illustrates key frames of the active contour’s evolution. The seed at the first iteration $i = 1$ includes three clusters of pixels at the defect edges, along with a sleeve of outlier pixels at the middle tow boundary. After 10 iterations, defective regions expand while outliers shrink and disappear. The texture-guided evolution effectively addresses noise due to its synthetic function, where both local and global forces act on the contour. The algorithm concludes at iteration 25, successfully converging to the defective region. In the final masked result, the algorithm isolates the defective region from the background (Fig. 4c).

TABLE II

SVM MODEL OPTIMIZED PARAMETERS AND PERFORMANCE EVALUATION.

Model Parameters		Performance Metrics	
Kernel constant (γ)	2^{-5}	Test accuracy	96.4 %
Penalty term (C)	2^{-3}	F1-score	96.43%
Feature extraction	72.7 ms	Precision	97.2 %
SVM prediction	17.0 ms	Recall	95.67%
Total time	89.7 ms		

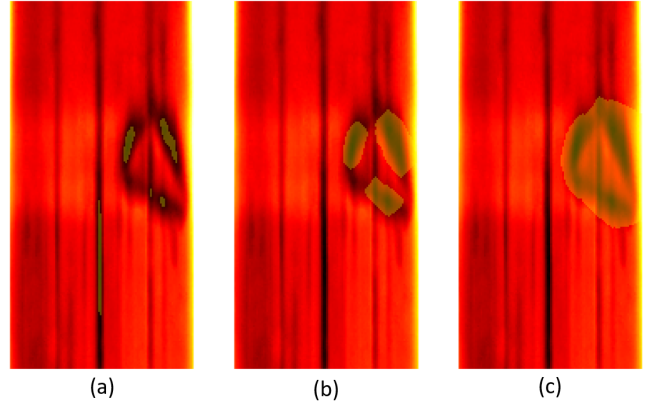


Fig. 4. Active contours with texture features: (a) initial seed mask at $i = 1$; (b) intermediate contour at $i = 10$; (c) final convergence at $i = 25$, isolating the defect region.

Although the shaded region contains a few peripheral pixels, introducing a slight positive bias in the defect area percentage metric values, this conservative approach minimizes the risk of false detection, ensuring system reliability. Thus, the algorithm is deliberately tuned for accurate yet conservative results.

Accurately comparing the performance of our algorithm with related studies is challenging in the absence of publicly available datasets for benchmarking, especially given the differences in methodologies across studies. However, we can provide a contextual evaluation of our model’s performance using results from similar studies with relatively close conditions. For example, [17] reported a mean segmentation IoU of 0.708 on 44 data instances where the evaluated defect area was defined as a bounding box around the defect. Similarly, [18] utilized deep learning to pixel-wise segment defect areas directly from point clouds of 43 lay-up images acquired using a laser profilometer, achieving a mean IoU of 0.776.

Our developed algorithm’s accuracy was evaluated using on 100 ground truth labeled images per defect class. The algorithm’s mean PA% is 93.2%, and IoU score is 0.72, indicating superior performance and high reliability in the thermography-based defect segmentation domain. It requires an average of 62.5 ms for 25 iterations. Despite higher computational demands, the active contours algorithm is preferred for its closed region identification and robustness. While limited to single-defect scenarios, it is sufficient for binary defect detection. Proper initialization, merging, and splitting techniques can extend its applicability to complex lay-ups.

C. AFP-DSS: A Case Study Evaluation

The developed AFP-DSS significantly enhances quality assessment and operator decision support in three key ways. Firstly, it derives a novel quantitative defect impact evaluation metric from the outcomes of system algorithms. Secondly, it features a continually expanding knowledge base, offering an evolving library of alert/recommendation pairs that cover an increasing range of manufacturing scenarios. Lastly, all results are presented to the operator in real-time through a graphical

user interface (GUI), facilitating automated thermal inspection and quality assessment of the lay-up.

We use a proof-of-concept illustration to rigorously evaluate the AFP-DSS within a realistic AFP production context, thereby assessing the system’s practicality and effectiveness (Fig. 5). The input is preprocessed and is then flagged as ‘Defective’ by the SVM classifier within the automated defect detection component. The defect region is subsequently segmented using the active contours algorithm, and the resultant region is highlighted on the image with a transparent mask. A bounding box provides location information about the defect on the lay-up image. Finally, the defect area percentage value is computed and presented for the system to find the best matching alert/recommendation pair in knowledge base.

The system combines qualitative attributes (defect shape, size, and location) with a quantitative defect impact evaluation. This feedback aids operators in assessing lay-up quality and making informed decisions. In this case study, a defect area percentage of 29.77% prompted the system to suggest halting the process and removing the foreign body. For narrower gaps, the recommendation might involve managing the defect while allowing the machine to continue, knowing that certain gaps and overlaps are corrected during the autoclave post-process. This approach significantly reduces time and effort for AFP process monitoring and quality inspection, enhancing efficiency and reliability. The system’s average execution time is 152.2 *ms*, meeting the real-time operation criterion of $\tau = 200$ *ms* per frame. Performance is expected to improve with hardware upgrades and optimized algorithms.

V. CONCLUSIONS AND FUTURE WORK

This study presents a novel framework for automated inspection and quality assessment of AFP systems, utilizing thermal imaging, machine learning, and computer vision. The system achieves high accuracy in defect detection and segmentation, reducing machine downtime and enhancing efficiency.

Future work will enhance the decision support system (DSS) by enriching the knowledge base and integrating machine learning, transforming it into a data-driven intelligent DSS

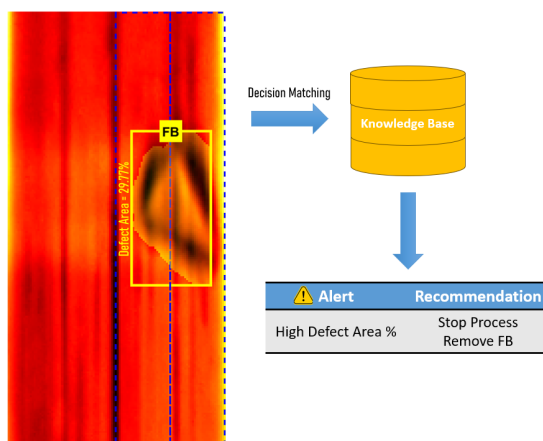


Fig. 5. Visual representation of the outcomes of the hybrid AFP process monitoring and quality inspection framework on a test case.

(AFP-IDSS). Additionally, we aim to extend the framework to handle variable stiffness and non-planar manufacturing processes.

ACKNOWLEDGMENT

The support provided by TUBITAK through the grant 218M715 is gratefully acknowledged.

REFERENCES

- [1] E. Oromiehie, B. G. Prusty, P. Compston, and G. Rajan, “Automated fibre placement based composite structures: Review on the defects, impacts and inspections techniques,” *Composite Structures*, vol. 224, p. 110987, 2019.
- [2] A. W. Blom, C. S. Lopes, P. J. Kromwijk, Z. Gurdal, and P. Camanho, “A theoretical model to study the influence of tow-drop areas on the stiffness and strength of variable-stiffness laminates,” *Journal of Composite Materials*, vol. 43, no. 5, pp. 403–425, 2009.
- [3] T. Rudberg, J. Cemenska, and E. Sherrard, “A process for delivering extreme afp head reliability,” *SAE International Journal of Advances and Current Practices in Mobility*, vol. 1, no. 2, pp. 333–342, mar 2019. [Online]. Available: <https://doi.org/10.4271/2019-01-1349>
- [4] E. Oromiehie, B. G. Prusty, G. Rajan, and P. Compston, “Optical fiber bragg grating sensors for process monitoring in advanced composites,” in *2016 IEEE Sensors Applications Symposium (SAS)*. IEEE, 2016, pp. 1–5.
- [5] B. Denkena, C. Schmidt, and P. Weber, “Automated fiber placement head for manufacturing of innovative aerospace stiffening structures,” *Procedia Manufacturing*, vol. 6, pp. 96–104, 2016.
- [6] E. D. Gregory and P. D. Juarez, “In-situ thermography of automated fiber placement parts,” *AIP Conference Proceedings*, vol. 1949, no. 1, p. 060005, 04 2018. [Online]. Available: <https://doi.org/10.1063/1.5031551>
- [7] C. Schmidt, T. Hocke, and B. Denkena, “Deep learning-based classification of production defects in automated-fiber-placement processes,” *Production Engineering*, vol. 13, pp. 501–509, 2019. [Online]. Available: <https://api.semanticscholar.org/CorpusID:115689102>
- [8] T. Yipeng, Q. Wang, H. Wang, J. Li, and Y. Ke, “A novel 3d laser scanning defects detection and measurement approach for automated fibre placement (afp) in-process inspection,” *Measurement Science and Technology*, vol. 32, 05 2021.
- [9] M. Zemzemoglu and M. Unel, “Design and implementation of a vision based in-situ defect detection system of automated fiber placement process,” in *2022 IEEE 20th International Conference on Industrial Informatics (INDIN)*, 2022, pp. 393–398.
- [10] —, “A hierarchical learning-based approach for the automatic defect detection and classification of afp process using thermography,” in *IECON 2023- 49th Annual Conference of the IEEE Industrial Electronics Society*, 2023, pp. 1–6.
- [11] I. S. Al-Mejibli, D. H. Abd, J. K. Alwan, and A. J. Rabash, “Performance evaluation of kernels in support vector machine,” in *2018 1st Annual International Conference on Information and Sciences (AiCIS)*. IEEE, 2018, pp. 96–101.
- [12] S. Meister, M. Wermes, J. Stüve, and R. Groves, “Review of image segmentation techniques for layup defect detection in the automated fiber placement process: A comprehensive study to improve afp inspection,” *Journal of Intelligent Manufacturing*, vol. 32, 12 2021.
- [13] A. Javed, A. U. Mirza *et al.*, “Comparative analysis of different fabric defects detection techniques,” *International journal of image, Graphics and Signal Processing*, vol. 5, no. 1, p. 40, 2013.
- [14] K. Sreeshan, R. Dinesh, and K. Renji, “Nondestructive inspection of aerospace composite laminate using thermal image processing,” *SN Applied Sciences*, vol. 2, no. 11, p. 1830, 2020.
- [15] T. F. Chan and L. A. Vese, “Active contours without edges,” *IEEE Transactions on image processing*, vol. 10, no. 2, pp. 266–277, 2001.
- [16] A. Felsberger, B. Oberegger, and G. Reiner, “A review of decision support systems for manufacturing systems,” *SAMI@ iKNOW*, p. 8, 2016.
- [17] A. Ghamisi, T. Charter, L. Ji, M. Rivard, G. Lund, and H. Najjaran, “Anomaly detection in automated fibre placement: learning with data limitations,” *Frontiers in Manufacturing Technology*, vol. 4, 2024.
- [18] Y. Tang, Q. Wang, L. Cheng, J. Li, and Y. Ke, “An in-process inspection method integrating deep learning and classical algorithm for automated fiber placement,” *Composite Structures*, vol. 300, p. 116051, 2022.